JOURNAL OF MATERIALS SCIENCE 16 (1981) 3489–3495

Electrical properties of $Bi_{80}Sb_{20}$ alloy thin films, vacuum-deposited at different substrate temperatures

V. DAMODARA DAS, N. MEENA
Thin Film Laboratory, Department of Physics, Indian Institute of Technology, Madras 600 036, India

Bismuth antimonide (composition 80:20) alloy thin films have been prepared by vacuum deposition at different substrate temperatures and, after annealing, their resistances have been recorded as a function of temperature, between 77 K and 500 K. The observed resistance against temperature behaviour of the films, and the effect of thickness and substrate temperature during deposition of the films, has been explained by considering that these films behave as semiconductors; the overlap between valence and conduction bands being removed due to the presence of antimony, the influence of a quantum size effect and the fact that the grain size of the films formed is a function of thickness and substrate temperature.

1. Introduction

The study of Bi, Sb and their alloys is interesting because of their semi-metallic behaviour, and the low Fermi energy and small effective mass of their conduction electrons. Bi and Sb are both group V elements, which have the same trigonal crystal structure and are completely soluble in each other in the solid state [1]. The addition of Sb to Bi does not alter either the crystal structure or the equality of positive and negative charge carrier concentrations [1, 2]. The change in the properties of Bi–Sb alloys and a transition from metallic to semiconducting behaviour arises because of the modification of the band structure (separation of bands) due to Sb addition. This is not the case for other Bi alloys like Bi–Pb and Bi–Sn, etc. where, as the added element belongs to a group other than group V, not only the band structure but also the equality of positive and negative charge carrier concentrations changes [2, 3]. The study of Bi–Sb alloys in the thin film state is especially interesting as the small effective mass of the conduction electrons and low Fermi energy mean that quantum size effects appear at small film thicknesses [4].

Many studies of the Bi–Sb alloys in the bulk and the thin film states have been made [2, 5–10]. Jain [2] considers that the pertinent part of the band structure of pure bismuth consists of a pair of light-mass bands at six symmetrically related positions in k-space (L-point bands) the upper of which is occupied by electrons, and a heavy-mass hole-band at two positions in k-space (T-point bands). The addition of antimony displaces the heavy-mass band downward with respect to the light-mass band causing a band gap and consequent semiconducting behaviour. Jain [2] has also shown that in Bi–Sb alloys, as the antimony concentration increases, the band overlap decreases until a band gap is formed (at 4 at% Sb) which increases until about 12 at% Sb and then gradually decreases until about 40 at% Sb, at which point band overlap again occurs, and hence, Bi–Sb alloys with Sb compositions between 4 at% and 40 at% exhibit semiconducting behaviour. Esaki [3] has also shown by tunnelling studies that, due to antimony addition, band overlap between the L-point conduction band and the T-point valence band in bismuth disappears and a band gap appears, and, with increasing antimony content in the alloy the band separation increases. Ramazanov [5], Petit *et al.* [7] and Kar [8] have studied the conductivity and mobility of Bi–Sb alloys in the thin film state for some compositions and temperature ranges. Damodara Das and Jagadeesh [9] have shown that

0022–2461/81/123489–07$02.70/0 © *1981 Chapman and Hall Ltd.*

even 1 at% Sb doped Bi alloys show semiconducting behaviour in the thin film state. In the present paper observations on Bi–Sb alloy thin films of composition $Bi_{80}Sb_{20}$ are discussed.

2. Experimental procedure

Bi–Sb alloy thin films of thicknesses between 35 nm and 600 nm were prepared by vacuum evaporation of bulk $Bi_{80}Sb_{20}$ alloy onto cleaned glass substrates, using a molybdenum boat, at various substrate temperatures (257 K, 298 K and 373 K). Before vacuum-depositing the Bi–Sb alloy films, thick (about 500 nm) silver contact films were deposited at the ends of the substrates and these substrates were mounted (one at a time) on a specially designed liquid N_2-cooled substrate holder inside the deposition chamber. The substrate temperature was varied by liquid N_2 circulation and an electrical heater provided in the substrate holder. The temperature was measured using a copper–constantan thermocouple. In order to ensure that the composition of the Bi–Sb alloy thin film formed was that of the starting bulk alloy ($Bi_{80}Sb_{20}$), films of different thicknesses were deposited individually in separate evaporations, by taking known quantities of the bulk alloy and completely evaporating the alloy in each deposition. The deposition rate also was kept high (about 5 nm sec^{-1}). After film deposition, the film and substrate were heated to 523 K and the film was annealed for 75 min at that temperature to homogenize the film and to remove the majority of the defects. The annealing temperature was chosen empirically by monitoring the resistance of the film during heat-treatment. Annealing above this temperature resulted in a rapid increase in resistance with temperature, attributed to discontinuities caused by grain growth and agglomeration in the films [11]. Similar determinations of annealing temperatures have been undertaken by Damodara Das and Jagadeesh in studying the annealing-out of defects in Sn–Sb alloy thin films [12–13]. It can can be said that annealing at 523 K causes only the removal of defects and no extensive grain growth. After the anneal, the film was cooled slowly from 523 K to room temperature during which time its resistance was continuously recorded *in situ* as the temperature decreased. The vacuum present during film formation, annealing and during the resistance measurements was about 2 to 4 $\times 10^{-5}$ torr. The source-to-substrate distance was 200 mm. Thickness and deposition rates were measured with a quartz crystal thickness monitor. Similar deposition conditions were maintained for films of different thicknesses formed at different substrate temperatures.

To verify the composition of the films formed, X-ray diffractograms of the films were taken. From the 2θ values of the two strong peaks [(0 0 3) and (0 0 6)] observed, a value of 1.1762 ± 0.0001 nm could be asigned to the c-parameter of the hexagonal lattice of the alloy. It has been shown [1] that the lattice constants of the Bi–Sb solid solution in the composition range 0 to 30 at% Sb vary linearly with Sb composition and are given by

$$a = 0.4546 - 23.84 \times 10^{-5}x \text{ nm} \quad (1)$$

and

$$c = 1.1863 - 51.66 \times 10^{-5}x \text{ nm}, \quad (2)$$

where x is atomic percentage of Sb. Thus, the calculated value of the c-parameter of the alloy $Bi_{80}Sb_{20}$ will be 1.1760 nm (from Equation 2), which is in agreement with the experimentally determined value of 1.1762 ± 0.0001 nm for the films. Thus, the composition of the film is that of the bulk alloy, $Bi_{80}Sb_{20}$. No evidence of the existence of any super-lattice structure or ordering was observed in the X-ray diffractograms of the thin films or in X-ray powder photographs of the bulk samples. Structural investigations by other researchers into Bi–Sb alloys also do not show any evidence of the existence of ordering or supper-lattice structure [1, 2, 6, 10].

3. Results

Fig. 1a, b and c show the variation of resistance with temperature of $Bi_{80}Sb_{20}$ alloy thin films of thicknesses between 35 and 600 nm, which were vacuum-deposited onto glass substrates at three different substrate temperatures (257 K, 298 K and 373 K) and annealed as detailed earlier. It is seen from Fig. 1 that the resistance of almost all the films decreases with an increase in temperature, thus exhibiting a negative temperature coefficient of resistivity (TCR) and hence non-metallic behaviour at low temperatures. At higher temperatures, the rate of decrease of resistance is lower, and practically zero for films of greater thicknesses. In the case of thicker films (of thicknesses about 250 nm), the resistance actually increases with increasing temperature, at high temperatures. It is also seen that the resistance of the film of a given thickness, formed at a higher

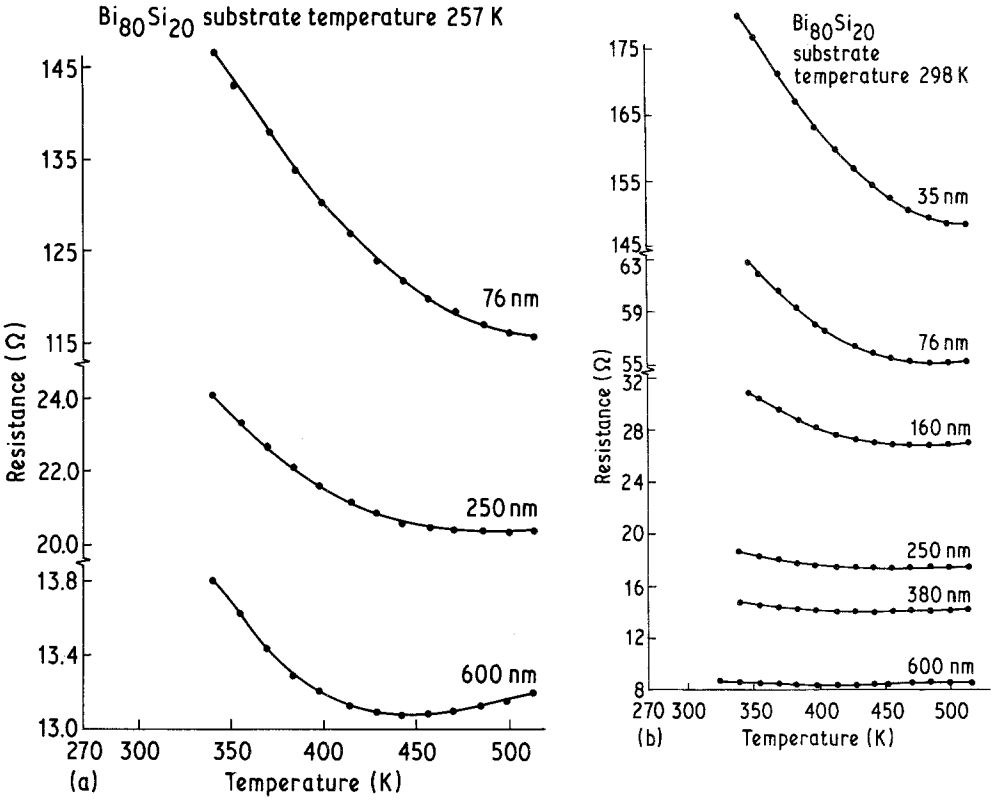

Figure 1 Resistance against temperature curves for $Bi_{80}Sb_{20}$ alloy thin films of different thicknesses vacuum-deposited at substrate temperatures of 257 K, 298 K and 373 K.

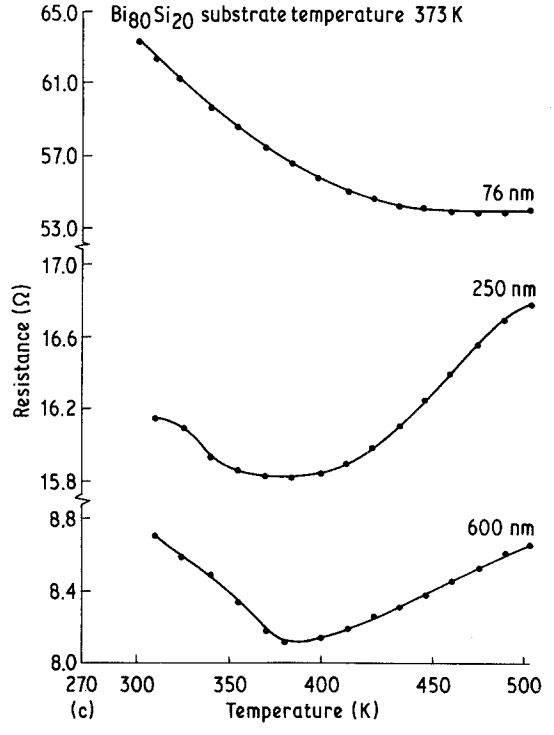

substrate temperature, is less than that of a film formed at a lower substrate temperature. For example, films of thickness 76 nm formed at 373 K, 298 K and 257 K have resistances at 500 K of approximately 54 Ω, 56 Ω, and 115 Ω; films of thickness 250 nm have resistances 16.8 Ω, 17.5 Ω, 20.2 Ω, while those of thicknesses 600 nm have resistances 8.7 Ω, 8.75 Ω and 13.15 Ω. This variation of resistance with substrate temperature is understandable because it is known from both nucleation theory [14] and experimentally [15] that films formed at higher substrate temperatures will have larger grain sizes and hence smaller grain-boundary areas. As mentioned earlier, the annealing temperature and duration were chosen so as to remove the majority of the defects without causing extensive grain growth and agglomeration. Hence, it can be considered that grain size and grain density of the film are not altered significantly by annealing, and the grain size of the films studied is a function only of the substrate temperature during deposition and film thickness. Thus grain-boundary effects will be fewer in the high

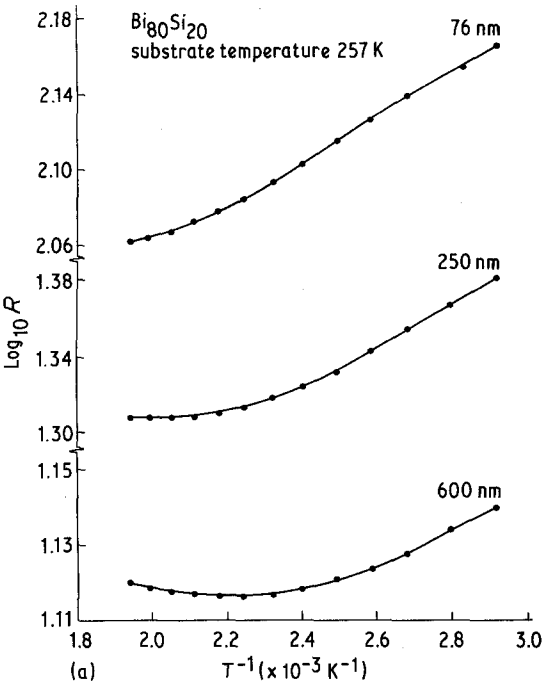

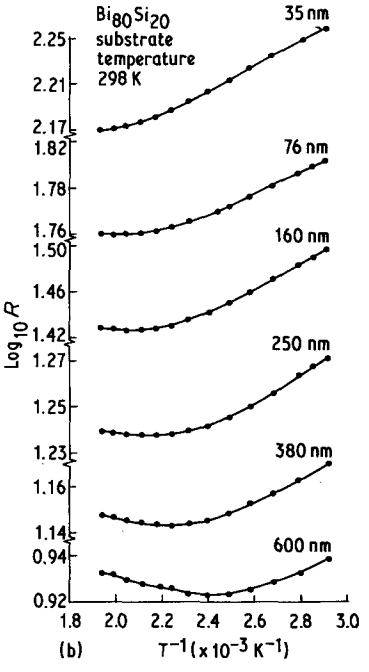

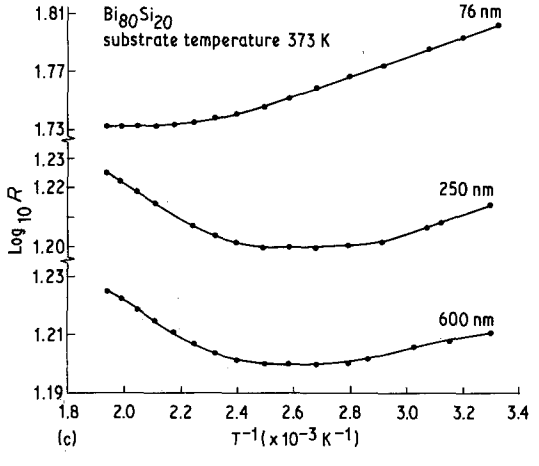

Figure 2 $\text{Log}_{10}R$ against T^{-1} plots for the films of Figure 1 in the high-temperature region.

substrate-temperature deposited film and, hence, it will exhibit a smaller resistance than a film deposited at lower substrate temperature.

Fig. 2a, b and c show the plots of $\log_{10}R$ against T^{-1} for the films of Fig. 1. It is seen from Fig. 2 that at low temperatures (between 300–450 K) $\log_{10}R$ against T^{-1} plots are linear for all the films indicating an activation mechanism. At higher temperatures (above 450 K), the resistance increases with increasing temperature showing normal metallic behaviour.

Fig. 3a and b show the plots of $\log_{10}R$ against T^{-1} in the low-temperature region, for three films of thicknesses 76 nm, 194 nm and 606 nm, formed at substrate temperatures 257 and 373 K. It is again seen that the resistance decreases with an increase of temperature in the whole region: in the high-temperature region (between 200 and 330 K), the plots are linear indicating another activation mechanism; at very low temperatures (near 77 K) the resistance slowly saturates at a high value. The behaviour is similar for all film thicknesses, but the saturation is attained at a higher temperature for the smaller thickness film.

Tables I and II give the activation energies calculated from the above two linear portions of $\log_{10}R$ against T^{-1} plots. It is seen from Table I that the activation energies in the high-temperature region decrease as the thickness increases for the films formed at all the three substrate temperatures. It is also seen that for a film of given thickness the above activation energy decreases as the substrate temperature increases. The activation energy in the low-temperature region (Table II) shows a tendency to decrease as the film thickness increases.

4. Discussion

The above observations, that the resistance of the films of different thicknesses first very slowly

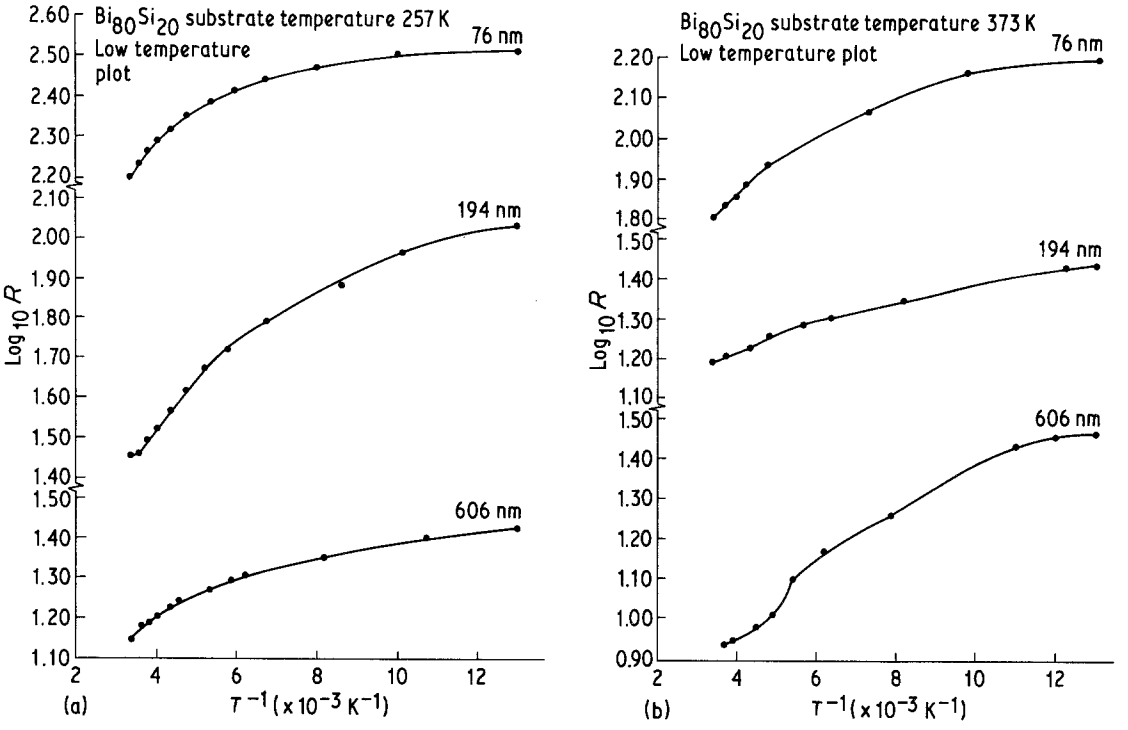

Figure 3 $Log_{10}R$ against T^{-1} plots for the films deposited at 257 K and 373 K in the low-temperature region.

decreases as the temperature is increased from 77 K, then at higher temperatures exponentially decreases with two different rates and, finally, at the highest temperature, increases linearly with increasing temperature, can be explained by dividing the entire temperature range into four regions.

(a) At the lowest temperatures, below 200 K, there is the saturation region due to impurity conduction.

(b) At higher temperatures, between 200 K and 300 to 330 K, there is the carrier generation region due to valence band–conduction band electronic transitions.

(c) There is the grain-boundary barrier activation region at still higher temperatures, between 300 to 330 K and 400 to 450 K.

(d) The normal metallic region, at the highest temperatures, i.e., above 400 to 450 K.

In Region a, at the lowest temperatures, the conduction is due principally to carriers generated by impurities and hence the resistance very slowly decreases with increase in temperature. In Region b carriers generated by valence band–conduction band transitions begin to play a dominant role in conduction and, as these carriers must be activated across the band gap, this is an activated process, and hence the resistance decreases exponentially

TABLE I Inter-grain barrier activation energies for $Bi_{80}Sb_{20}$ alloy thin films

Thickness (nm)	Barrier energies* (meV)		
	Substrate temperature 257 K	Substrate temperature 298 K	Substrate temperature 373 K
35	–	21.1	–
76	25.4	18.7	13.4
160	–	22.2	–
250	23.4	12.5	6.9
380	–	10.8	–
600	9.8	8.0	4.0

*Barrier energies are accurate to ± 1 meV.

TABLE II Band gap values for $Bi_{80}Sb_{20}$ alloy thin films

Thickness (nm)	Band gap* at two substrate temperatures (meV)	
	Substrate temperature 257 K	Substrate temperature 373 K
76	44.4	38.3
194	52.2	18.1
606	31.3	23.9

*Band gap energies are accurate to ± 2 meV.

with increasing temperature. The activation energy values evaluated from the linear plots of the $\log_{10}R$ against T^{-1} curves in Region b (Table II) thus represent the band gap values. In Region c, at still higher temperatures, the conduction is still activated, as $\log_{10}R$ against T^{-1} plots in this region are also linear and resistance decreases with increase in temperature. This could possibly be due to the effect of grain boundaries in the film. As the created charge carriers have to pass from one grain to the next, overcoming the intergrain boundaries, these boundaries can be considered as barriers which have to be overcome for conduction to occur. Thus, the activation energies evaluated in this region are possibly inter-grain barrier energies (Table I). Finally, in Region d, at the highest temperatures, the resistance increases with increase in temperature, as in the case of a normal metal, due to increased thermal scattering.

The above model presupposes that the material behaves as a semiconductor, even though bismuth is metallic in the bulk state because of overlapping conduction and valence bands. It has been shown by Sandomirskii [4], Lutski *et al.* [16] and others [17] that bismuth behaves as a narrow band-gap semiconductor in the thin film state below a particular thickness, due to the emergence of a quantum size effect. It has also been shown by Jain [2] and others [3], as mentioned earlier, that even in the bulk state, addition of antimony to bismuth removes the conduction band–valence band overlap, making it behave as a semiconductor for antimony compositions between 4 and 40 at %. In the thin film state the antimony addition removes the overlap, and the quantum size effect leads to further separation of bands [9]. Thus, the $Bi_{80}Sb_{20}$ alloy films behave as narrow band-gap semiconductors due to antimony addition and the emergence of quantum size effect.

The fact that the band-gap values observed in the present films (Table II) are larger than those reported for the same material in the bulk state [1] and the observation that the band gap is a function of thickness showing a tendency to decrease with increasing thickness, indicate the influence of quantum size effect on band separation. The separation of bands due to the quantum size effect is inversely proportional to t^2, where t is the thickness [4, 18], and, hence, the contribution to band separation due to the quantum size effect will decrease as the thickness increases. Hence, the overall band separation will decrease as the thickness increases.

It is interesting to note that the activation energy values in Table I decrease as the thickness increases and also as the substrate temperature during deposition increases. This observation lends support to the assumption that these activation energies could be grain-boundary barrier energies. This is because, as is well known [14, 15], the thin films formed at higher substrate temperatures have larger grains, and as the films become thicker, the individual grains also become bigger. Thus, thicker films and high substrate temperature films have larger-sized grains compared to the thinner films and those formed at low substrate temperatures. If it is considered that the inter-grain barrier activation energy (barrier height) is a function of grain size, decreasing with increasing grain size, we would expect the barrier height to decrease as the substrate temperature and thickness increase, as has been observed. Thus, all the observations made can be satisfactorily explained by dividing the entire temperature region into four regions, as described above.

5. Conclusions

It has been concluded from the study of $Bi_{80}Sb_{20}$ alloy thin films formed at different substrate temperatures that these films exhibit semiconducting behaviour. This behaviour is attributed to the removal of overlap between valence band and conduction band due to antimony addition and the emergence of a quantum size effect. Activated conduction observed at higher temperatures is attributed to inter-grain barriers. The decrease in the barrier height with increasing thicknesses and higher substrate temperature is attributed to the increased grain size of these films.

Acknowledgements

The authors are thankful to Dr M. S. Jagadeesh for experimental assistance.

References

1. W. B. PEARSON, "Handbook of Lattice Spacings and Structures of Metals and Alloys" Vol. 2 (Pergamon Press, Oxford and New York, 1967) p. 719.
2. A. L. JAIN, *Phys. Rev.* **114** (1959) 1518.
3. L. ESAKI, *J. Phys. Soc. Japan* **21** (1966) Suppl. 89.
4. V. B. SANDOMIRSKII, *Sov. Phys. JETP* **25** (1967) 101.
5. K. A. RAMAZANOV, *Sov. Phys. Sol. Stat.* **3** (1962) 1640.
6. H. J. GOLDSMID, *Phys. Status Solidi (a)* **1** (1970) 7.
7. J. L. PETIT and C. R. BEBOL, *Scand. Acad. Sci.* **B272** (1971) 211.
8. R. K. KAR, *Nucl. Phys. Sol. Stat. Phys.* (India) **14C** (1972) 140.
9. V. DAMODARA DAS and M. S. JAGADEESH, *J. Vac. Sci. Technol.* **19** (1981) 89.
10. M. S. JAGADEESH, PhD thesis, Indian Institute of Technology, India, 1977.
11. L. I. MAISSEL, in "Handbook of Thin Film Technology" edited by L. I. Maissel and R. Glang (McGraw-Hill Book Co., New York, 1970) pp. 13–30.
12. V. DAMODARA DAS and M. S. JAGADEESH, *Thin Solid Films* **24** (1974) 203.
13. *Idem, J. Phys. Chem. Solids* **38** (1977) 167.
14. C. A. NEUGEBAUER, in "Physics of Thin Films" Vol. 2, edited by G. Hass and R. Thun (Academic Press, New York, 1964) p. 1.
15. K. L. CHOPRA, "Thin Film Phenomena" (McGraw-Hill Book Co., New York, 1969) p. 183.
16. V. N. LUTSKI and T. N. PINSKER, *Thin Solid Films* **66** (1980) 55.
17. YU. F. OGRIN, V. N. LUTSKI and M. I. ELINSON, *Sov. Phys. JETP Lett.* **6** (1967) 58.
18. V. DAMODARA DAS and N. JAYAPRAKASH, *Vacuum* **31** (1981) 133.

Received 19 March and accepted 8 June 1981.